

Performance of Metal-free Organic Dyes with Complementary Absorption in Zinc Oxide Dye-sensitized Solar Cells

G.R.A. Kumara^{1,2}, L.Y. Rangali², E. N. Jayaweera², C. S. K. Ranasinghe², and R.M.G Rajapakse^{1,2}

¹Department of Chemistry. University of Peradeniya, Peradeniya, Sri Lanka

² Postgraduate Institute of Science. University of Peradeniya, Peradeniya, Sri Lanka

Abstract

Dye-sensitized solar cells (DSCs) are fabricated using two metal-free organic indoline dyes, D131 and D149, which have complimentary absorption bands in the visible region and hence have extended light absorption, which are adsorbed individually and both together, on ZnO mesoporous, interconnected semiconductor nanoparticles. The thickness of the ZnO mesoporous layer and the molar ratio of the two dyes in the dye adsorption solution are optimized to get the best DSC performance. The optimized cell of configuration FTO/ZnO buffer layer/ZnO mesoporous layer/dye/electrolyte/Pt-FTO gives the power conversion efficiency of 4.19% under AM 1.5 solar radiation, for the dye adsorbed from the mixture of D131 and D149 in 1:1 molar ratio. Increased light absorption in by the two dyes gives highest J_{sc} . Electrochemical impedance studies reveal that the electron life time of co-sensitized DSC is higher than that of the DSC sensitized with only D149 indicating lesser recombination in the former cell.

Keywords: Zinc Oxide, D131, D149, Dye-sensitized solar cell, metal-free organic dyes.

1. Introduction

Dye-sensitized solar cells (DSCs) are considered to be technology between second and third generation solar cells and they were first reported by Grätzel and co-workers in 1991 [1]. In comparison with the conventional Si-based solar cells, the attractive properties of DSCs are their simple manufacturing processes, much lower cost, flexibility, lightness and low toxicity [2, 3]. A DSC is composed of dyed, interconnected, nanoparticulate matrix of a semiconductor deposited on electronically conducting glass surface to act as photoanode, a liquid electrolyte containing a redox couple and a counter electrode. Both the efficiency and the cost of DSCs are determined by the nature of the each part of the DSC. As such, research into improvement of

each and every part of DSC is essential to increase its efficiency and to decrease production cost.

A meso-porous, interconnected, nanoparticulate TiO_2 semiconducting layer dyed by a suitable dye that absorbs in the visible region of the electromagnetic spectrum is used as the working electrode of the most efficient DSCs. TiO_2 has several different crystal forms which include rutile, anatase and brookite. Rutile is the thermodynamically most stable form of TiO_2 . The band gaps of rutile, anatase and brookite are 3.0 eV, 3.4 eV and 3.3 eV, respectively [4], and hence these semiconductor matrices do not absorb in the visible region. However, dyes capable of absorbing in the visible region are adsorbed on to semiconductor nanoparticulate surfaces for excited dye molecules to inject electrons to the conduction band of the semiconductor particles. The semiconductor particles act as a carrier of electrons helping to transport through random diffusion towards the back contact conducting glass surface. Though the highest efficiencies are still given by the TiO_2 semiconductor, many other semiconductor materials such as ZnO, SnO_2 and Nb_5O_2 have been investigated though the efficiencies obtained are far below that of TiO_2 based DSCs [5].

ZnO is an alternative semiconductor that has been used instead of TiO_2 in DSCs. The band gap of ZnO is same as that of TiO_2 anatase but ZnO has higher electron mobility and electron diffusion coefficient than TiO_2 . However, the lower efficiency of ZnO based DSCs is due to increased recombination of injected electrons with oxidized dye molecules or the oxidized species of the redox couple. As such, the best power conversion efficiency that has been obtained for ZnO is 5% [6] which is much less than that of TiO_2 . Recent reports have established that TiO_2 based DSCs can be fine-tuned to get over 10 % efficiency [7]. Despite all these drawbacks, ZnO is still anticipated as a good alternative to TiO_2 due to the fact that highly

crystalline ZnO with different morphologies such as nanoparticles, nanowires [8], nanorods, nanotubes [9], nanoflowers, nanosheets, and branched nanostructures can be easily synthesized for testing in DSCs [10]. Another advantage of ZnO is that the nanoparticles of ZnO can be sintered at relatively lower temperatures such as 350 °C to have interconnected nanoparticles attached to fluorine-doped SnO₂ (FTO) conducting surfaces as demonstrated in this work.

The isoelectric point (the point of zero charge) of a metal oxide is defined as the pH at which the concentration of protonated and deprotonated surface groups are equal [10]. The isoelectric point of ZnO is ~ 9 and that of TiO₂ is ~ 6 [11]. As a result, when the ZnO is immersed in Ru-complex dyes which containing several carboxylic acid groups, ZnO will be dissolved. Due to the dissolution of surface atoms of ZnO, a thick layer of agglomerated Zn²⁺/dye complexes are formed making it difficult to have a monolayer dye coverage on ZnO surfaces. This effect also contributes to the lower efficiencies of ZnO based DSCs containing ruthenium dyes which containing two or four carboxylic acid groups in their molecules. This effect can be reduced if indoline dyes are used since these dye molecules contain only one carboxylic acid group which is used to anchor dye molecules to ZnO surfaces [12]. Indoline dyes have another advantage they have much higher molar absorption coefficients than those of ruthenium based dyes resulting in higher light absorption by the former dyes [13]. Since most of these dyes absorb only a part of the visible spectrum, the use of complimentary dyes which absorb in different regions of the spectrum would enable the harvesting of the entire visible spectrum to improve conversion efficiency.

In this work, we have constructed interconnected ZnO nanoparticle based DSCs containing Indoline D131 or D149 dyes adsorbed separately and also absorbed in combination using a solution containing different molar ratios of the two dyes and their conversion efficiencies were determined. We show below the co-adsorption of the two dyes on ZnO surfaces gives higher conversion efficiency in DSCs than when they are separately adsorbed. This manuscript also contains extensive characterization of the materials and their applications in DSCs.

2. Experimental

2.1 Fabrication of Dye-sensitized Solar Cells

ZnO powder (Kanto Chemical, Japan, 1.70 g), ethanol (Hayman, England, 99.9%) (50.0 ml), and distilled water (50.0 ml) were mixed by vigorous stirring and acetic acid was added drop-wise until a clear solution is obtained which is termed as dense layer solution. Half of FTO glass plates were covered by using thermo tapes. Then the dense layer solution was sprayed onto a cleaned FTO glass plates at 250 °C to obtain transparent dense layers with a sheet resistance in the range of 250 Ω cm⁻¹ to 300 Ω cm⁻¹.

Then, commercial ZnO (Kanto Chemical, Japan, 20 nm, 0.6 g), acetic acid (Wako Chemicals, Japan, 99.7%) (6 drops), Triton X-100 (Wako Chemicals, Japan) (4 drops) were ground in motor and ethanol (Hayman, England, 99.9%) (60.0 ml) was added to the mixture. Then the resulting suspension was ultrasonicated for 10 min. This ZnO colloidal solution was sprayed onto the ZnO dense layer on cleaned FTO glass plates at 150 °C. By varying the volume of ZnO colloidal solution, thin films of thicknesses 9 μm, 12 μm, 15 μm and 18 μm were prepared. They were then sintered at 350 °C for 30 min in air. Then they were left to cool down up to about 80 °C and placed in 0.3 mM dye in acetonitrile/tert-butyl alcohol mixture (v/v = 1:1 for 12 h. Dyes used were Indoline dyes D131, D149 and their mixtures. The dye solutions were characterized by UV-Visible Absorption Spectroscopy. DSCs were prepared with the configuration of FTO/ZnO dense layer/ ZnO mesoporous layer/dye/electrolyte/Pt-FTO electrode. The liquid electrolyte used was composed of 0.1 M LiI, 0.05 M I₂, 0.6 M dimethylpropylimidazolium iodide dissolved in acetonitrile.

FTO/ZnO dense layer and FTO/ZnO dense layer/ZnO mesoporous layer films prepared were extensively characterized by X-ray Diffractometry (XRD). Photovoltaic properties of the DSCs fabricated were determined by irradiating AM 1.5 simulated solar light. The DSCs were also characterized for their electrical and transport properties with the aid of AC impedance analysis. The EI analysis of the DSCs were performed over the frequency range of 100 kHz to 0.01 Hz under dark with forward bias condition at the applied bias

voltage set at the open circuit voltage of DSCs (-0.550 V) using an AC voltage amplitude of 10 mV.

3. Results and Discussion

3.1 Optimization of DSCs as a function of thickness of the mesoporous ZnO layer

Variation of the photovoltaic characteristics of DSCs at different ZnO mesoporous film thicknesses sensitized by D131 and D149 are depicted in Table 1.

Table 1: Photovoltaic parameters of the DSCs with different thicknesses of mesoporous ZnO films sensitized by D131 and D149 dyes

Dye	thickness / μm	Photovoltaic parameters				
		I_{sc}/mA	$J_{sc}/\text{mA cm}^{-2}$	V_{oc}/V	FF	$\eta/\%$
D131	6	1.63	6.54	0.537	0.65	2.29
	9	1.88	7.52	0.564	0.67	2.85
	12	2.19	8.78	0.536	0.69	3.25
	15	2.81	11.25	0.522	0.63	3.71
	18	2.33	9.31	0.534	0.66	3.29
D149	6	1.65	6.60	0.556	0.57	2.09
	9	1.71	6.86	0.552	0.74	2.80
	12	2.37	9.51	0.553	0.67	3.50
	15	2.79	11.14	0.530	0.62	3.67
	18	2.64	10.55	0.553	0.62	3.47

As revealed by the data shown in Table 1, optimum thickness of the ZnO mesoporous layer to produce most efficient DSC is 15 μm for both D131-sensitized and D149-sensitized DSCs. As for TiO_2 -based DSCs sensitized by indoline dyes, best performance is observed at much lesser mesoporous layer thickness (3 μm) than those containing ruthenium based dyes (12 – 14 μm) [14]. This is due to the fact that indoline dyes have much higher molar absorption coefficients (D131, 53000 $\text{M}^{-1}\text{cm}^{-1}$ and D149, 68700 $\text{M}^{-1}\text{cm}^{-1}$) than those of ruthenium based dyes (N3, 13900 $\text{M}^{-1}\text{cm}^{-1}$ and N719, 15000 $\text{M}^{-1}\text{cm}^{-1}$). It has been shown that from dye adsorption measurements that TiO_2 mesoporous layers have much higher porosity than the porosity of ZnO mesoporous layers. Therefore, in order to get the same amount of dye coverage in ZnO layers much higher thickness is required. This is manifested by our results where 15 μm of mesoporous thickness is needed to give the best performance. Increasing the thickness beyond this optimum value results in increased recombination of injected electrons thus lowering the conversion efficiency.

3.2 J-V characteristics of DSCs

The photocurrent density-voltage (J-V) characteristics for DSCs constructed using 15 μm -thick ZnO photo-electrode films sensitized with D131 or D149 dyes and different molar ratios of the dye mixtures are reported in Table 2. According to the J-V characteristics of DSCs, the optimized power conversion efficiencies of 3.71%, 3.67%, 4.19%, 3.68% and 3.42% are achieved for DSCs under AM 1.5 solar radiation, for D131, D149, dye mixture of D131 and D149 (1:1 molar ratio), dye mixture of D131 and D149 (2:1 molar ratio) and dye mixture of D131 and D149 (1:2 molar ratio). Corresponding J-V characteristics for ZnO-based DSCs sensitized with the above dyes/dye mixtures are shown in Fig.1.

Table 2: Photovoltaic parameters for the ZnO-based DSCs sensitized with D131 dye, D149 dye, dye mixture of D131 and D149 (1:1 molar ratio), dye mixture of D131 and D149 (2:1 molar ratio) and dye mixture of D131 and D149 (1:2 molar ratio) under AM 1.5 irradiation.

Dyes/ Dye mixtures	I_{sc} /mA	J /mA cm^{-2}	V_{oc} /V	FF	η /%
D149	2.79	11.14	0.530	0.62	3.67
D131	2.81	11.25	0.522	0.63	3.71
D149:D131(1:1)	3.06	12.23	0.547	0.63	4.19
D149:D131(1:2)	2.73	10.92	0.522	0.65	3.68
D149:D131(2:1)	2.60	10.41	0.538	0.61	3.42

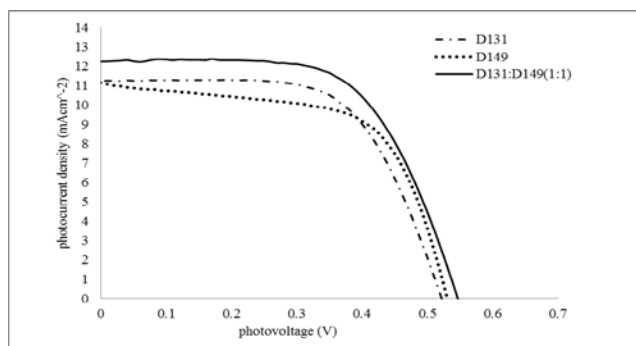


Fig. 1 J-V characteristics of DSCs sensitized with only D131 dye, D149 dye and both D131 and D149 (1:1 molar ratio) under AM 1.5 irradiation.

Although there is adequate literature to support to fact that the power conversion efficiencies of D131-sensitized DSCs are lesser than those sensitized with D149 dye, we observed higher conversion efficiency for DSCs sensitized with D131 than those sensitized with D149 dye under otherwise identical conditions [15]. This may be due to the differences in surface coverage of different dyes. Since D131 dye molecule is smaller in size than D149 dye molecule [Fig. 2 (a) and (b)] it is possible that D131 molecules are capable of penetrating even smaller pores of the ZnO film than D149 dye molecules giving rise to higher

surface coverage by D131 dye molecules. This may result in higher electron injection by D131 molecules than D149 molecules under identical conditions.

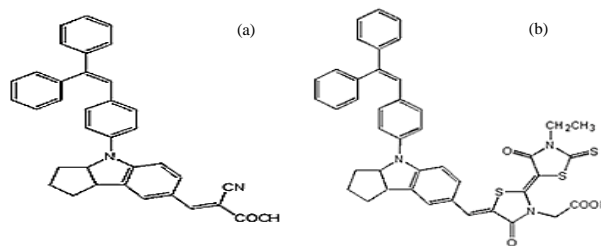


Fig. 2 Molecular structure of (a) Indoline D131 dye and (b) Indoline D149 dye.

To determine the optimum molar ratio of co-sensitization by the two dyes DSCs were fabricated by adsorbing dyes mixtures of D131 and D149 with three different molar ratios (1:1, 2:1 and 1:2) and their photovoltaic performances were determined. The best power conversion efficiency is observed for the ZnO film sensitized by the dye mixture containing D131 and D149 at 1:1 molar ratio (4.19%) which is significantly higher than that of the DSCs sensitized by individual dyes and also those co-sensitized with two dyes adsorbed onto ZnO mesoporous layer at 1:2 and 2:1 molar ratios of the two dyes.

Although, D149-sensitized device shows lower efficiency than D131 sensitized one, the molar absorption coefficient of D149 ($68700 M^{-1} cm^{-1}$) is higher than that of D131 dye ($53000 M^{-1} cm^{-1}$). As can be seen from the absorption spectra of individual dyes at 0.30 mM concentration and that of the dye mixture with 1:1 molar ratio in the same concentration of each dye (Fig. 3) it is very clear that D149 absorbs in a wider range of the visible spectrum than D131 and the mixture covers almost entire visible range one contrasting the other. It is interesting to note that the absorption spectrum of the 1:1 mixture of the dyes each at the same concentration as that of individual dyes is same as the additive absorption spectrum of the two dyes. This shows that the two types of molecules in the solution do not interact with each other and hence do not undergo any aggregation. The same can be expected when the two dyes are adsorbed on to the surfaces of mesoporous ZnO particles and hence the two dyes adsorb in complementary manner not competing for

the same site on ZnO surfaces. This is very important for monolayer coverage by the two dyes and to prevent dye aggregation thus giving the best efficiency when the two are adsorbed from a solution containing 1:1 molar of the two dyes.

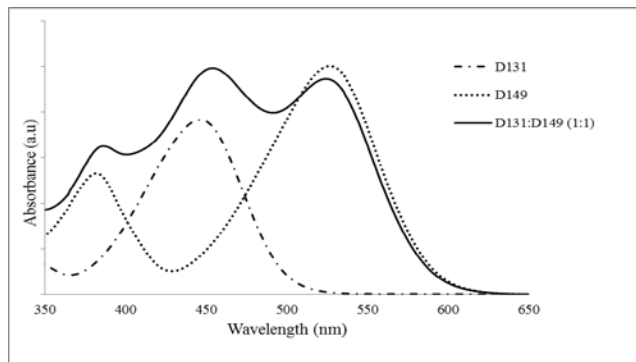


Fig. 3 The optical absorption spectra for only D131 dye, D149 dye and both D131 and D149 (1:1 molar ratio) dye solutions.

3.3 X-Ray Diffraction (XRD) studies

XRD patterns of the ZnO dense layer on FTO and ZnO porous layer on this dense layer are depicted in Fig. 4. The diffraction peaks observed at 2θ values of 31.88° , 34.56° , 36.28° , 47.62° , 56.52° , 63° , and 67.8° for the latter are characteristic of the hexagonal Wurtzite structure of ZnO (JCPDS card No. 05-0664). The latter has more intense diffraction peaks than former obviously due to the fact that more ZnO is present in the latter than former. In the XRD pattern of the dense ZnO layer on FTO only the prominent peaks at 2θ values of 31.88° , 34.56° , 36.28° , and 56.52° , 63° . It is interesting to note that even the FTO/Dense ZnO layer does not show peaks due to FTO. This is because the FTO surface is fully covered by at least 50 nm thick dense ZnO layer without any pinholes. Such a dense layer is very important in DSCs to prevent the recombination of electrons that are diffused to the FTO/Dyed ZnO/Electrolyte triple junction. Since both diffraction patterns contain only the diffractions from ZnO planes it can be inferred that both ZnO layers do not contain any crystalline impurities or even other crystallographic phases of ZnO apart from the Wurtzite phase.

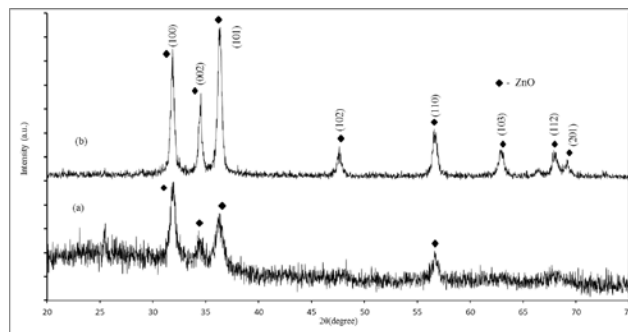


Fig. 4 XRD pattern of (a) ZnO dense layer on FTO glass plate and (b) ZnO porous layer present on the dense layer deposited on FTO glass plate.

The mesoporous ZnO film consists of particles in nano scale range as indicated by a definite line broadening of the XRD peaks. The diameter of the particles in ZnO mesoporous layer, d , can be calculated using Debye-Scherrer formula given in Equation 1.

$$d = 0.89\lambda / (\beta \cos \theta) \quad (1)$$

where 0.89 is Scherrer constant, λ is the wavelength of X-ray and is 0.154062 nm, θ is the Bragg diffraction angle, and β is the full-width at half maximum of the diffraction peak corresponding to plane (101). Thus an average particle size of the ZnO mesoporous layer calculated in this way is 20 nm which is derived from the full-width at half maximum of the most intense peak corresponding to (101) plane located at 36.28° . This is a magnificent coincidence since the average particle size of the ZnO particles used here is also 20 nm. This shows that ZnO particles are not aggregated in the solution or even when they are deposited on the surfaces of the particles in the ZnO dense layer. This means that discrete ZnO particles are deposited in the ZnO porous layer and are interconnected by the calcination. Such a structure is of vital importance for fabricating DSCs.

3.4 Electrochemical Impedance Studies of the DSCs

Electrochemical impedance spectroscopy is used to understand the charge transport properties and to

estimate the electron lifetime (τ_e) for the DSCs sensitized with D131 and D149 individually and as a mixture at 1:1 molar ratio and corresponding Nyquist plots are shown in Fig. 5. Electron lifetimes (τ_e) of these ZnO-based DSCs can be calculated using equation 2.

$$\tau_e = R_{rec} C_{\mu} \quad (2)$$

Where, τ_e is electron lifetime, R_{rec} is the recombination resistance and C_{μ} is the chemical capacitance.

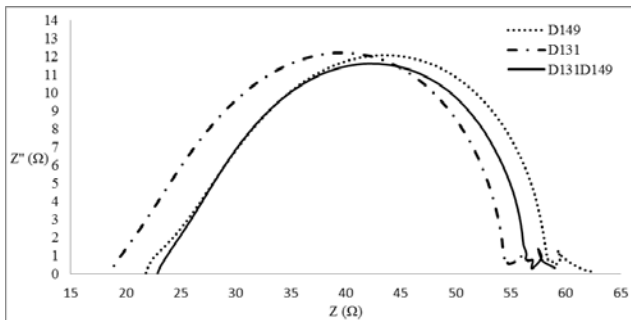


Fig. 5 Nyquist plots of the impedance spectra of DSCs sensitized with only D131 dye, D149 dye and both D131 and D149 at 1:1 molar ratio.

Electron lifetime (τ_e) of the DSCs sensitized by individual dyes and both together follow the trend D131 > D131: D149 (1:1) > D149, as depicted in Table 3. Higher electron lifetime indicates effective suppression of the back reaction. Electron lifetime of D149-sensitized device is lower than that of other two devices. This is manifested by the poor performance of the D 149 sensitized DSC. Generally, D149 dye molecules have a tendency to aggregate on ZnO surface and this aggregation can be prevented by using aggregate preventers such as deoxycholic acid [16]. We have used indoline D131 dye which can perform dual functions; as co-absorbent that can be excited upon visible light irradiation and inject electrons to the CB of ZnO particles and also as an aggregate preventer. This aggregation prevention is achieved by D131 dye molecules occupying the free spaces on the ZnO nanoparticles and hence not providing space for D 149 molecules to aggregate. This might be the reason for higher electron lifetime for the device co-sensitized device than that of D131 sensitized device.

Table 3: Calculated electron lifetimes for the ZnO-based DSCs sensitized individually with D131 and D149 dyes and as a mixture at 1:1 molar ratio.

Dye	R_{rec}/Ω	$C_{\mu} \times 10^{-2} / F$	τ_e / ms
D149	34.7	91.1	3.16
D131	33.1	113	3.74
D131:D149 (1:1)	32.2	113	3.64

4. Conclusions

In this work, we have prepared ZnO based DSCs sensitized by D 131 or D 149 dyes individually and both together. For the dual-sensitization, the molar ratios of the two dyes was varied and the best performance was observed for the device in which dye absorption was carried out from a dye solution containing 1:1 molar ratio of the two dyes; D131 and D149. This gives an overall conversion efficiency of 4.19% with J_{SC} , V_{OC} and FF of 12.23 mA cm⁻², 0.547 V and 0.627, respectively. Calculated electron life times (τ_e) for DSCs sensitized with D131, D149 and D131 and D149 (1:1) molar ratio are 3.74 ms, 3.16 ms and 3.64 ms, respectively. As a result of the recombination prevention, the power conversion efficiency of the dual-sensitized device is higher than that of the DSC sensitized with only D149.

Acknowledgments

This work is supported by the National Science Foundation of Sri Lanka (NSF/Fellow/2011/02).

References

- [1] B. O'Regan, M. Grätzel, A low cost, high efficiency solar cell based on dye- sensitized colloidal TiO₂ films, Nature 353 (1991) 737.
- [2] A. Mishra, M. K. R. Fischer, P. Bauerle, Metal-Free Organic Dyes for Dye-Sensitized Solar Cells: From Structure: Property Relationships to Design Rules, Chem. Int. Ed., 48 (2009) 2474.

- [3] L. M. Goncalves, V.D.Z. Bermudez, H. A. Ribeiro and A. M. Mendes, Dye-sensitized solar cells: A safe bet for the future, *Energy Environ. Sci* 1 (2008) 655.
- [4] M. Landmann, E. Rauls and W. G. Schmidt, The electronic structure and optical response of rutile, anatase and brookite TiO₂, *J. Phys.: Condens. Matter* 24 (2012) 195503 (6pp).
- [5] M. Grätzel, Solar Energy Conversion by Dye-Sensitized Photovoltaic Cells, *Inorg. Chem.* 44 (2005) 6841.
- [6] K. Keis, E. Magnusson, H. Lindstrom, Sten-Eric Lindquist, A. Hagfeldt, A 5% efficient photoelectrochemical solar cell based on nanostructured ZnO electrodes, *Sol. Energy Mat. Sol. Cells* 73(2002) 51.
- [7] Y. Chiba, A. Islam, Y. Watanabe, R. Komiya, N. Koide and L. Han, Dye-sensitized solar cells with conversion efficiency of 11.1%, *J. J. of Applied Physics*, 45 (2006) 24-28.
- [8] J. B. Baxter, E. S. Aydila, Nanowire-based dye-sensitized solar cells, *Appl. Phys. Lett.* 86 (2005) 053114
- [9] A. B. F. Martinson, J. W. Elam, J. T. Hupp, M. J. Pellin, ZnO Nanotube Based Dye-Sensitized Solar Cells, *Nano Lett.* 7 (2007) 2183.
- [10] Q. Zhang, C. S. Dandeneau, X. Zhou, G. Cao, ZnO Nanostructures for Dye-Sensitized Solar Cells, *Adv. Mater.* 21 (2009) 4087.
- [11] J. A. Anta, E. Guillén, R. Tena-Zaera, ZnO-Based Dye-Sensitized Solar Cells, *J. Phys. Chem. C* 116 (2012) 11413.
- [12] Y. Ren, Y.-Z. Zheng, J. Zhao, J.-F. Chen, W. Zhou, X. Tao, A comparative study on indoline dye- and ruthenium complex-sensitized hierarchically structured ZnO solar cells, *Electrochemistry Communications* 16 (2012) 57.
- [13] M. Ye, X. Wen, M. Wang, J. Icozzia, N. Zhang, C. Lin, Z. Lin, Recent advances in dye-sensitized solar cells: from photoanodes, sensitizers and electrolytes to counter electrodes, *Materials Today* 18 (2015) 155.
- [14] T. Hiriuchi, H. Miura, K. Sumioka and S. Uchida, *J. Am. Chem. Soc.* 126 (2004) 12218-12219.
- [15] R. Jose, A. Kumar, V. Thavasi, K. Fujihara, S. Uchida, S. Ramakrishna, Relationship between the molecular orbital structure of the dyes and photocurrent density in the dye-sensitized solar cells, *Appl. Phys. Lett.* 93 (2008) 023125.
- [16] S. Ito, H. Miura, S. Uchida, M. Takata, K. Sumioka, P. Liska, P. Comte, P. Peckys and M. Grätzel, High-conversion-efficiency organic dye-sensitized solar cells with a novel indoline dye, *Chem. Commun.* (2008) 5194-5196.